GeoConvention 2015
GEOSCIENCE
new horizons
Telus Convention Centre • 4-8 May 2015 • Calgary, AB Canada

High Speed Calculation of Reflectivity From Arbitrary Anisotropic Interface

Reza Malehmir, Douglas R. Schmitt
University of Alberta

Summary

Ignoring the elastic anisotropy in the Earth causes many artifacts in seismic processing and interpretation**.** To date, these issues have been ameliorated by using approximations to the full solutions for wave propagation and reflectivity for special material symmetries. A Matlab™ based program algorithm has been written to extend these capabilities to the general case of reflectivity from the interface between two anisotropic slabs of arbitrary symmetry and orientation. To achieve this, the algorithm solves for polarization, amplitude and slowness of all the wave modes generated by a plane wave incident to the interface. In the first step, the plane-wave velocities and polarizations of all three orthogonal wave modes are calculated for a given incidence angle. Second, the algorithm determines the reflection and transmission angles of all of the possible scattered modes followed by their respective velocities and polarization vectors. With this information, the algorithm solves system of equations incorporating the imposed boundary conditions to arrive at the scattered wave amplitudes. We have tested this algorithm in deliberately non-realistic and actual cases to make sure that there is no energy leakage in the system of calculations. This algorithm is can be applied to the processing, imaging, and inversion of seismic data in anisotropic media.

Introduction

In this paper we introduce our algorithm which is able to calculate plane-wave reflectivity from any anisotropic interface which separates two anisotropic media without any limit on type of anisotropy in either side of the interface. Most real cases in the Earth are not horizontal transverse isotropy (HTI) and will be tilted TI or even more complex. Solution for reflectivity in complex anisotropic media is highly non-linear and complicated, hence many researchers have tried to linearize the solution by introducing assumptions about type of anisotropy on each side of interface.. Readers can follow up in Thomsen (1988, 1986) that linearized Daley and Hron's (1977) solution using 'weak boundary contrast' assumption. Ruger (1997, 1998), Ursin and Haugen (1996) as well as various other authors extended this approach for PP (P-wave incident and reflected) approximation in weak elastic anisotropy and weak boundary contrast in TI and orthorhombic media. In this contribution we developed algorithm which is able to solve for reflectivity in most complex interface separating two unconditional anisotropic media. The algorithm is able to solve for wave polarization, slowness and amplitude ratios of all wave modes generated from a welded interface bounding two homogenous anisotropic slabs of arbitrary symmetry and orientation. A variety of tests of the algorithm with complex situations are presented to illustrate its capabilities and reliability.

Theory

To calculate plane-wave properties in anisotropic medium the algorithm starts with Musgrave (1970) and Rokhlin et al (1986) who used the full elastic wave (Equation 1) and its plane-wave solution (Equation 2).

$$\rho \ddot{u} = c_{ijkl} \frac{\partial u_k}{\partial x_j} \left(\frac{\partial u_k}{\partial x_l} + \frac{\partial u_l}{\partial x_k} \right), \qquad (1)$$

$$u = \chi \xi e^{-ik(nr - vt)}, \qquad (2)$$

where *x*, ρ and ***c*** are direction, density and stiffness matrix of the media, respectively. Hooke's law relates stress ($\boldsymbol{\sigma}$) to strain ($\boldsymbol{\varepsilon}$) with stiffness matrix, $\boldsymbol{\sigma}_{ij} = c_{ijkl}\, \boldsymbol{\varepsilon}_{kl}$. Also $\chi, \xi, \boldsymbol{n}$, *v* and *k* are the amplitude, the polarization direction, the vector normal to the plane wave front, the phase velocity, and the wave number of the plane-wave. Considering continuity of momentum and inertia yields a stiffness matrix with 21 elastic parameters, which dictates the anisotropic behavior of the medium. In the lowest symmetry of triclinic, twenty one elastic parameters are required. However as we increase the symmetry in the medium, this number drops to 11, 9, 5 and 2 for monoclinic, orthorhombic, transversely isotropic and isotropic, respectively (see Schmitt (2015) for a recent discussion of this). By substituting the plane-wave solution (Equation 2), into the wave equation (Equation 1) we reach to the equation known as Christoffel-Kelvin(Equation 3).

$$[\Lambda_{ik} - \rho v^2 \delta_{ik}] \xi_k = 0; \; i, k = 1,2,3.$$

$$\Lambda_{ik} = c_{ijkl}\, n_j n_l \qquad (3)$$

where δ is Kronecker delta operator. For a given raypath, ***n***, nontrivial solution shows three independent phase velocities and polarizations for three wave modes with orthogonal polarizations known as one quasi-longitudinal (qP) and two quasi-shear waves (qS1and qS2).

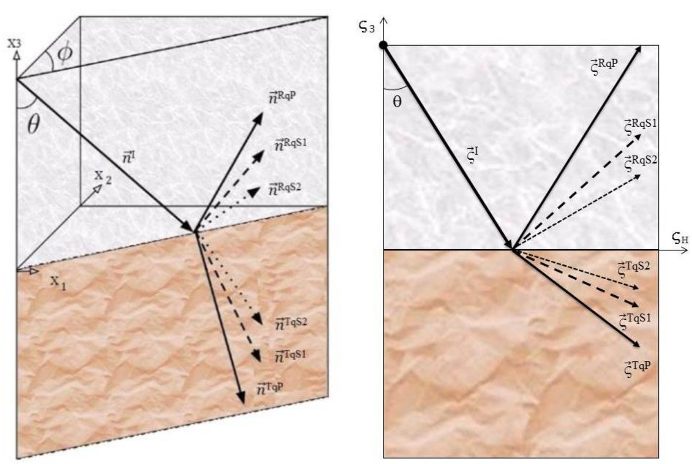

a b

Figure 1: (a) Schematic geometry of plane-wave generation from an interface separating two anisotropic media and incident wave with incidental direction of θ and azimuthal direction of ϕ, (b) 2D representation along azimuthal direction of ϕ in slowness domain, showing that horizontal slowness of generated wave modes are equal to horizontal slowness of incident wave.

Our algorithm uses this step to solve for v and ξ of the incident wave. We must then find the direction of the reflected and transmitted waves from the interface. To find the directions of the generated waves, continuity of the displacement at the interface is used to find its slowness vector. To satisfy this condition, horizontal slowness of the generated wave modes must be equal to horizontal slowness of the incident wave, and for vertical slowness, algorithm solve 2 to find appropriate vertical slowness. Having direction of generated waves, speed and polarization of each wave mode is calculated using procedure explained at the beginning of this section. Now we have all the information about the ray paths generated from the anisotropic interface, except amplitude ratios. The algorithm then employs two major boundary conditions at the interface: the continuity of traction force (τ) and the conservation of displacement (Equation 4).

$$\sum_{\alpha=1}^{3}\chi^{\alpha}\zeta^{\alpha}{}_{i} + \sum_{\alpha=4}^{6}\chi^{\alpha}\zeta^{\alpha}{}_{i} = \chi^{I}\zeta^{I}{}_{i}$$

$$\sum_{\alpha=1}^{3} c_{ijkl}{}^{U}\chi^{\alpha}\eta_{j}\,\varsigma_{k}^{\alpha}\,\zeta^{\alpha}{}_{i} + \sum_{\alpha=4}^{6} c_{ijkl}{}^{L}\chi^{\alpha}\eta_{j}\,\varsigma_{k}^{\alpha}\,\zeta^{\alpha}{}_{i} = c_{ijkl}{}^{L}\chi^{I}\eta_{j}\,\varsigma_{k}^{I}\,\zeta^{I}{}_{i} \qquad (4)$$

where $\boldsymbol{\eta}$ is normal to the boundary and the superscripts U and L indicate the upper and the lower mediums, respectively. Further details of these calculations including a Matlab™ program may be found in Malehmir and Schmitt (2015). In example section, we test our algorithm by solving for the reflectivity from the interfaces between arbitrary two anisotropic media.

Examples

In this section we will show results from the algorithm solve amplitude ratios of all generated wave modes from some of the most difficult anisotropic boundaries. To test the algorithm strength in energy balancing, we tested our algorithm with virtual boundary inside a water tank, where on both sides the same water exists. By looking at the results from the algorithm, as one could expect, there is no energy leakage form the boundary and the whole energy is transmitted. Other examples which are discussed here are, Isotropic-HTI boundary, then extend it to interfaces with Isotropic-Orthorhombic, and finally a complex boundary separating Monoclinic-Triclinic, after Bass (1995), figure 2. Interested readers can refer to Malehmir and Schmitt (2015) for more examples and details regarding the algorithm.

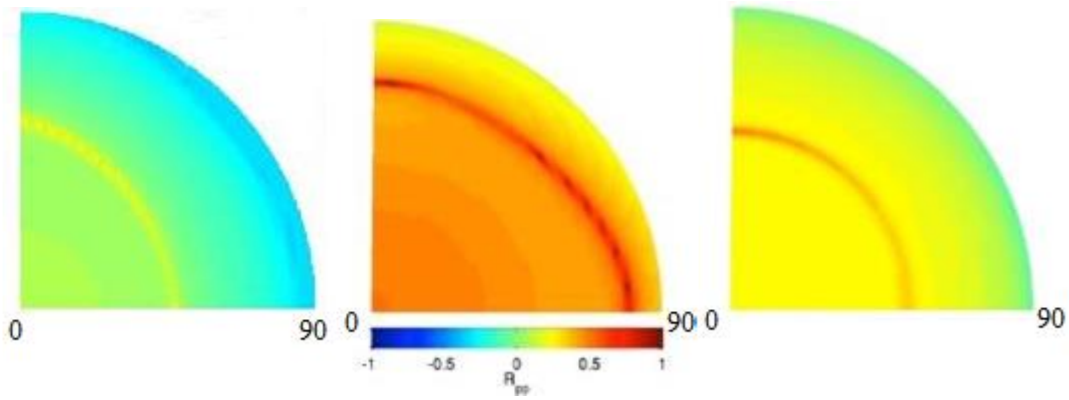

a. b. c.

Figure 2: Calculated PP reflectivity from an between (a) Isotropic-HTI contact, (b) an Isotropic-Orthorhombic contact, and (c) and Monoclinic-Triclinic contact with an incident angle and azimuthal direction from 0 to 90 degrees. High temperature ribbon indicates the critical angle reflection.

Conclusions

In this paper we developed a unified algorithm to solve for plane-wave reflectivity from an arbitrary anisotropic interface. The algorithm starts with calculation of key properties of all wave-modes in the homogenous medium such as slowness and polarization. Then, algorithm continues to find amplitude ratios of all generated wave modes from the interface by satisfying logical boundary conditions. We tested the algorithm with several scenarios in order to study precision of the calculation and energy leakage at the interface. This algorithm is capable of handling models with strong low symmetry anisotropic media up to triclinic anisotropy. This algorithm is free from any non-realistic assumption and is not limited to any type of anisotropy. Future works will be dedicated to apply this algorithm in seismic data migration and inversion to achieve higher quality images from the anisotropic Earth.

Acknowledgements

The authors thank Natural Science and Engineering Research (NSERC) and Canada Research Chair program to support of this project of Experimental Geophysics Group (EGG) at the University of Alberta.

References

Bass, J., 1995. Elasticity of Minerals, Glasses, and Melts. AGU Reference Shelf.

Daley, P. F., and Hron, F., 1977. Reflection and transmission coefficients for transversely isotropic media. Bulletin of the Seismological Society of America, 67(3), 661–675.

Malehmir, R., and Schmitt, D. R., 2015, An Algorithm to Calculate the Seismic Reflectivity and Transmissivity of General Anisotropic Structures, Computer and Geoscience, (*Submitted*).

Musgrave, M. J. P., 1970. Crystal Acoustics: Introduction to the Study of Elastic Waves and Vibrations in Crystals (p. 288). Holden-Day.

Rokhlin, S., Bolland, T., & Adler, L. (1986). Reflection and refraction of elastic waves on a plane interface between two generally anisotropic media. The Journal of the Acoustical Society of America, 79(4), 906–918.

Rüger, A., 1997. P -wave reflection coefficients for transversely isotropic models with vertical and horizontal axis of symmetry. Geophysics 62 (3), 713–722.

Rüger, A., 1998. Variation of P-wave reflectivity with offset and azimuth in anisotropic media. Geophysics 63 (3), 935–947.

Schmitt, D.R., 2015, Seismic Properties, in Vol. 11: Geophysical Properties of the Near Surface Earth: 'Treatise on Geophysics', 2nd Edition, ed. G. Schubert, pp. 44, in press, 2015.

Schoenberg, M.; and J. Protazio; 1992, "Zoeppritz" rationalized and generalized to anisotropy: Journal of Seismic Exploration, 1, 125–144.

Thomsen, L., 1986. Weak elastic anisotropy. Geophysics 51 (10), 1954–1966.

Ursin, B., & Haugen, G. (1996). Weak-contrast approximation of the elastic scattering matrix in anisotropic media. Pure and Applied Geophysics, 148(3-4)